

Green O-RAN Operation: a Modern ML-Driven Network Energy Consumption Optimisation

Xuanyu Liang*, Ahmed Al-Tahmeesschi*, Swarna Chetty* and Hamed Ahmadi*

*School of Physics Engineering and Technology, University of York, United Kingdom

Abstract—The increasing energy demand of next-generation mobile networks, especially 6G, is becoming a major concern—particularly due to the high power usage of base station components Radio Units (RUs), which often remain active even during low traffic periods. To tackle this challenge, our study focuses on improving energy efficiency in Open Radio Access Network (O-RAN) systems using intelligent control strategies. Twin Delayed Deep Deterministic Policy Gradient (TD3) leverages a continuous action space to overcome the limitations of traditional discrete-action methods like Deep Q-Learning Network (DQN). By avoiding exponential growth in action space, TD3 enables more precise control of RU sleep modes in dense and large radio environments. Simulation results show that our approach consistently achieves over 50% energy savings compared to the always-on baseline, with TD3 outperforming DQN-based methods by up to 6%, while also offering better stability and faster convergence.

Index Terms—6G, Energy Efficiency (EE), Sleep Mode, O-RAN, DQN, TD3

I. INTRODUCTION

To accommodate the rapidly increasing demand for mobile traffic, Base Stations (BSs) have been widely deployed to satisfy user data rate requirements. Although dense deployments of BSs significantly enhance network capacity and ensure better coverage and connectivity, they also lead to substantial energy consumption. Approximately 80% of the energy consumption in mobile cellular networks is attributed to BSs. The increase in energy consumption not only amplifies operational costs for wireless network providers but also contributes to an increase in CO₂ emissions [1]. Consequently, addressing energy efficiency in BS operations is becoming increasingly crucial. Traditional BS designs often feature integrated hardware with limited flexibility, making it difficult to manage and optimize energy use effectively. Such integrated designs limit the ability to selectively activate or adjust the power levels of individual components, resulting in a continuous and frequently inefficient energy consumption.

In this context, the O-RAN introduces a novel architecture that disaggregated traditional BS functionalities into three key components: the Central Unit (CU), the Distributed Unit (DU), and the RU and the integration of open interfaces and standards [2], [3]. This architectural change allows for more granular control over network functionality, enabling better scalability, easier upgrades, and more targeted energy-saving measures. By hosting the CU and DU functions in the cloud and simplifying the role of the RU to focus on lower-layer physical processing and RF tasks, O-RAN enables a more flexible and resource-efficient deployment. Another key innovation in O-RAN is the introduction of the RAN

Intelligent Controller (RIC), which addresses various operational dynamics through its two main components: the Near Real Time RIC (Near-RT RIC) and the Non Real Time RIC (Non-RT RIC). In this paper, we focus on the development and deployment of xApps within the Near-RT RIC. xApps are modular, third-party applications that run on the Near-RT RIC platform and enable real-time, policy-driven control of radio resources.

The energy consumption of RUs represents a significant fraction of the overall energy used by cellular networks, particularly in dense 5G deployments [4]. Although RUs are primarily deployed to handle peak traffic demands, their continuous operation during periods of low traffic results in substantial energy wastage. To mitigate this inefficiency, dynamically switching off lightly-loaded RUs—a strategy commonly referred to as sleep mode has emerged as an effective energy-saving approach [5]–[8]. For example, [6] introduced a random sleep mode mechanism for BSs in small cell networks, while [7] proposed a sequential algorithm to deactivate BSs with minimal network impact while meeting mobile rate requirements. Additionally, [8] presented several schemes for deactivating macro BSs in heterogeneous networks, maintaining the original coverage performance by adjusting the transmission power of the remaining active macro BSs and incorporating additional micro BSs. Although mathematical optimization techniques have proven effective in enhancing network energy efficiency, their application in complex scenarios, with an increasing number of BSs and multi-objective constraints, can become computationally intensive and time-consuming.

In this context, Machine Learning (ML) approaches have been proposed to reduce energy consumption in complex and dynamic wireless networks while preserving the User Equipment (UE) Quality of Service (QoS) [9]–[12]. In particular, both [11] and [9] introduce ML-based strategies tailored for ultra-dense networks. In [11], an Long Short-term Memory (LSTM)-based deep neural network is employed to extract temporally correlated features from channel information, thereby enabling the dynamic switching on/off of BSs. In contrast, [10] utilizes a DQN to optimize the sleep mode of BSs and incorporates an action selection network to reduce the action space by filtering invalid actions. Moreover, [9] proposes an actor-critic Deep Reinforcement Learning (DRL) approach that addresses the challenges posed by large action spaces without relying on explicit action space reduction, while also predicting future traffic arrivals to improve decision-making accuracy.

In this paper, we propose a TD3-based algorithm to optimize

RU sleep mode decisions for improved energy efficiency in large and dense O-RAN environments. Specifically, we design and implement the TD3 model as an xApp that operates based on real-time user activity patterns, rather than relying on static traffic snapshots as in prior work [13]. By utilizing a continuous action space, TD3 avoids the exponential growth in action combinations that occurs with traditional discrete-action methods when the number of RUs increases, enabling scalability in complex network settings. For comparative evaluation, we introduce two variants of Deep Q-Network (DQN) as baseline models: DQN-Multiple Action (DQNMA) and DQN-Single Action (DQNSA). Simulation results demonstrate that the TD3 model achieves greater energy savings and faster convergence than both DQN-based approaches. Furthermore, unlike DQNMA, which becomes infeasible in large-scale deployments due to action space explosion, the TD3 model remains stable and effective even in extended and complex network areas.

The main contributions of this paper are:

- We develop a TD3-based DRL algorithm for optimizing the sleep mode strategy of RUs in O-RAN. The proposed model is implemented as an xApp, enabling low-latency, data-driven control over RU activation states.
- To establish a comparative baseline, we also develop two DQN variants: DQNMA, which simultaneously controls all RUs, and DQNSA, which updates one RU at each time step to reduce action space complexity.
- We demonstrate that the TD3 model consistently outperforms the DQN-based approaches in both energy savings and convergence speed.

II. SYSTEM MODEL

In this section, we discuss the system model of O-RAN environment. We consider the downlink transmission where M RUs equipped with a single antenna serve K UEs. Each RU is served by a corresponding DU and DUs are connected with single CU. In addition, UEs move at a speed v , choosing from 0 to v_{max} . Note that, in our study, the UEs move within the area and do not leave it. The sets of RUs and UEs are represented as $\mathcal{M} = \{1, 2, \dots, M\}$ and $\mathcal{K} = \{1, 2, \dots, K\}$ respectively. We also introduce the α_m which is a binary variable to indicate the active/sleep of RU m . Here $\alpha_m = 1$ means the RU m is in active mode, otherwise $\alpha_m = 0$.

In our work, each RU is able to provide a total of Q_m Physical Resource Blocks (PRBs) to the UEs associate to the RU. Let U_m^t denote the total number of UEs associate with RU m at time slot t . On top of that, we denote $n_{m,k}^t$ is the number of PRBs allocated to the k^{th} UE in RU m . Therefore, the total number of PRBs usage N_m^t of RU m at time slot t can be computed as $N_m^t = \sum_{u=0}^{U_m^t} n_{m,k}^t$. Based on this, the RU load at time slot t is defined as:

$$l_m^t = \frac{N_m^t}{Q_m}. \quad (1)$$

In our work, we consider the fading channel model from the RU m to the UE k as $h_{m,k}$. Therefore the Signal-to-Noise Ratio (SNR) $SNR_{m,k}$ of the k^{th} UE associate to the RU m at time t is presented as :

$$SNR_{m,k} = \frac{P_{TX} h_{m,k} \frac{n_{m,k}}{Q_m}}{n_{m,k} N_0}, \quad (2)$$

where P_{TX} is the maximum transmission power of an RU and the transmission power allocated to the UE depends on the percentage of PRBs occupancy. The denominator corresponding to additive white Gaussian noise. The corresponding data rate of UE k is given by:

$$R_k^t = n_{m,k} B * \log_2(1 + SNR_{m,k}), \quad (3)$$

where B is the bandwidth of each PRB

A. Power Consumption Model and Problem Formulation

The power consumption of RU is divided into three parts. The first part is the fixed power P_m^{Fix} of RUs consumed by the signal processing, cooling system and power supply, which only varies depending on the active/sleep mode of RU. Then the load dependent power comes from the Power Amplifier (PA) P_m^{data} . The load in this paper is represented by the PRB usage as shown in (1), and transition power P_m^{trans} is generated when the mode of the base station changes, e.g. from sleep mode to active mode. Combining these three parts, the power consumption of the RU m at time slot t is:

$$P_m^t = P_m^{Fix,t} + P_m^{data,t} + P_m^{trans,t}. \quad (4)$$

First, fixed power of RU m consumed by the active or sleep mode is given by:

$$P_m^{Fix,t} = \alpha_m^t P_m^{active} + (1 - \alpha_m^t) P_m^{sleep}, \quad (5)$$

where P_m^{active} and P_m^{sleep} are represented the fixed power consumption of RU m in active mode and sleep mode, respectively. Then, the transmission power of RU m which is scaled with load of RU m at time slot t computed as:

$$P_m^{data,t} = \alpha_m^t \frac{P_{TX}}{\eta} * l_m^t = \alpha_m^t \frac{P_{TX}}{\eta} * \frac{N_m^t}{Q_m}, \quad (6)$$

where $\eta \in [0, 1]$ is the power amplifier efficiency of the RU m . P_{TX} here is the constant value and only scale with the percentage of the load. Therefore, the more UEs are associated the more power consume. Last but not least, the transition power of RU m is given by:

$$P_m^{trans,t} = \max(\alpha_m^t - \alpha_m^{t-1}, 0) \cdot V_m^{trans} \quad (7)$$

where, α_m^{t-1} is the active/sleep mode of RU m in the last time slot. V_m^{trans} is the power consumed by switching on and off mode of the RU m . The transition power P_m^{trans} is only consumed when the RU is switched on.

Finally, the total power consumption of the entire network in time slot t is defined as:

$$\begin{aligned} P_{tot}^t &= \sum_{m=1}^M (P_m^{Fix,t} + P_m^{data,t} + P_m^{trans,t}) \\ &= \sum_{m=1}^M (\alpha_m^t P_m^{active} + (1 - \alpha_m^t) P_m^{sleep}) + \alpha_m^t \frac{P_{TX}}{\eta} * \frac{N_m^t}{Q_m} \\ &\quad + (\max(\alpha_m^t - \alpha_m^{t-1}, 0) \cdot V_m^{trans}) \end{aligned} \quad (8)$$

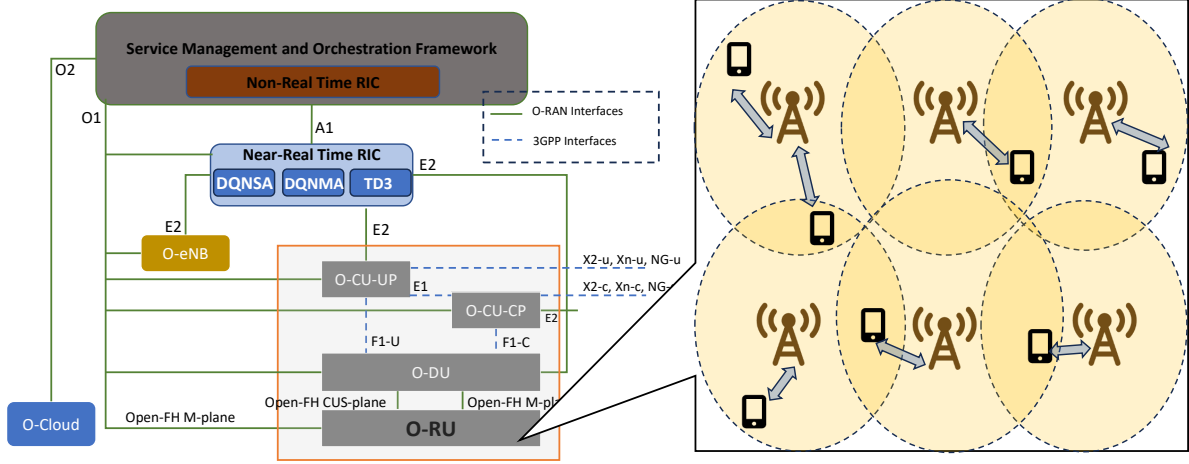


Fig. 1: shows O-RAN Architecture, with components and interfaces from O-RAN and 3GPP. O-RAN interfaces are drawn as solid lines, 3GPP ones as dashed lines. The layout of the O-RU is shown in the picture in the right section.

We assume all the RUs are in active at the initial stage when $t - 1 = 0$. Therefore, the power minimization problem can be formulated as follow:

$$\begin{aligned} \mathcal{P}_1 : \quad & \min_{\{\alpha_m^t, n_{m,k}^t\}} \sum_{t=1}^T P_{tot}^t \\ \text{s.t.} \quad & R_k^t \geq R_{k,min}^t, \quad \forall k \in \mathcal{K}, \forall t \in \mathcal{T} \\ & N_m^t \leq Q_m^t, \quad \forall m \in \mathcal{M}, \forall t \in \mathcal{T} \\ & \alpha_m^t \in \{0, 1\}, \quad m \in \mathcal{M}, \forall t \in \mathcal{T}, \end{aligned} \quad (9)$$

where $R_{k,min}^t$ is the minimum data rate requirement of UE k at time interval t . The second constraint is that the allocated PRBs need to be within the total number of PRBs and $\mathcal{T} = \{1, 2, \dots, T\}$.

III. ENERGY EFFICIENCY DRL BASED SOLUTION

The primary objective of this study is to optimize the sleep and active modes of BS in dynamic radio environments to minimize network-wide energy consumption without impacting the UEs QoS. In this section, we proposed a solution combined with TD3 algorithm, an advanced actor-critical Reinforcement Learning (RL) framework to optimize the sleep mode strategy.

A. Markov Decision Process Problem

To solve the sleep mode optimization problem which is the NP-hard problem, we decompose the original problem into Markov Decision Process (MDP) problem. In this subsection, we discuss the state space, action space, and reward function of TD3 model to consist the MDP problem.

State Space: state comprises essential information used for policy training. At each time step t , it contains the real data rate of the UE, represented as $\mathbf{R}^t = [R_1^t, R_2^t, \dots, R_K^t]^T$, which captures the system's ability to meet user demands. The RU operation mode from the previous time step are denoted as $\boldsymbol{\alpha}^{t-1} = [\alpha_1^{t-1}, \alpha_2^{t-1}, \dots, \alpha_M^{t-1}]^T$. The PRB utilization of the RUs is given by $\mathbf{L}^t = [l_1^t, l_2^t, \dots, l_M^t]^T$,

quantifying the load on the RUs. Finally, the spatial positions of the UEs in the network are represented as: $\mathbf{U}^t = [(x_1^t, y_1^t), (x_2^t, y_2^t), \dots, (x_K^t, y_K^t)]^T$, characterized by their (x, y) coordinates, providing insight into UE distribution and mobility. In summary, the state can be expressed as:

$$s_t = [\mathbf{R}^t, \boldsymbol{\alpha}^{t-1}, \mathbf{L}^t, \mathbf{U}^t]^T.$$

All state parameters are normalized to facilitate a better interpretation by the agent.

Action Space: TD3 addresses a fundamental limitation of conventional discrete-action methods such as DQN. In such methods, the size of the action space increases exponentially with the number of BSs, scaling as 2^M . For instance, in a system with 12 RUs, there would be 2^{12} potential sleep/active state combinations, making exploration computationally infeasible. In contrast, TD3 employs a continuous action space, which scales linearly with the number of RUs. So in TD3, action $\alpha \in \mathcal{A}$ represents the binary operational states of all RUs, defined as:

$$\mathcal{A} = [\alpha_1, \alpha_2, \dots, \alpha_M].$$

Each element α_m corresponds to an RU, where $\alpha_m = 1$ denotes that the RU is active, and $\alpha_m = 0$ indicates that the RU is in sleep mode. These actions are derived from the output of the TD3 model, which guides the energy-efficient operation of the network.

Reward Function : reward $r \in \mathbb{R}$ is designed to balance energy efficiency and user satisfaction, guiding the model towards an optimal operational policy. It is defined as:

$$r = -w_1 \cdot \frac{P_{tot}}{P_{max}} - w_2 \cdot \frac{K_{unsat}}{K},$$

where P_{max} corresponds to the energy consumption if all RUs are all active. The term K_{unsat} denotes the number of users with data rates below their required thresholds, normalized by the total number of users K . The weights w_1 and w_2 adjust the relative importance of energy efficiency and user satisfaction.

Normalization is used in the reward function to ensure that the contributions of energy consumption and user satisfaction are scaled to comparable ranges.

B. Energy efficiency TD3 solution in O-RAN

In this work, we utilize a customized version of TD3 to dynamically control the sleep/active states of RUs in an O-RAN network, aiming to minimize energy consumption while ensuring UE QoS. Unlike generic applications of TD3, our approach explicitly encodes the physical behavior of base station sleep transitions and the spatio-temporal dynamics of user distribution into the RL framework as shown in Algorithm 1.

In our problem, the action space corresponds to a binary vector representing the states of all RUs. The TD3 actor network outputs a continuous vector $\mu_\theta(s) \in [0, 1]^n$. This continuous output is then discretized by a thresholding function f_d , such that the final action vector is:

$$a = f_d(\mu_\theta(s) + \eta_n), \quad a_i = \begin{cases} 1 & \text{if } \mu_\theta(s)_i + \eta_i > 0.5 \\ 0 & \text{otherwise} \end{cases}$$

where $\eta_n \sim \mathcal{N}(0, \sigma^2)$ is temporally-decayed Gaussian exploration noise. This design allows the actor to learn a *soft preference* over base station activation while the environment enforces hard switching decisions.

The environment is modeled to reflect practical conditions, including dynamic user mobility, soft handovers, and energy consumption computation. Each transition (s, a, r, s') is collected into a replay buffer. To mitigate overestimation bias, TD3 employs twin Q-networks Q_{ϕ_1}, Q_{ϕ_2} . In our setting, this is particularly important because suboptimal base station activations may seem energy-efficient but degrade user satisfaction. The critic update targets are computed as: $y = r + \gamma \min_{i=1,2} Q_{\phi_i}(s', f_d(\mu_{\theta'}(s') + \epsilon))$ where ϵ is clipped noise added for *target policy smoothing*, encouraging robustness to small perturbations in base station decisions. This is crucial in our environment due to the discrete switching and spatial sensitivity of user association.

The actor network is updated with the deterministic policy gradient using the critic feedback, $\nabla_\theta J(\theta) = \mathbb{E}_{s \sim \mathcal{D}}[\nabla_a Q_\phi(s, a)|_{a=\mu_\theta(s)} \cdot \nabla_\theta \mu_\theta(s)]$. To improve training stability, we follow the TD3 principle of delayed policy updates, updating the actor and target networks only every steps, allowing the critics to stabilize before policy updates influence the network topology. We also implement *soft updates* for the target networks: $\theta' \leftarrow \tau\theta + (1-\tau)\theta'$, $\phi'_i \leftarrow \tau\phi_i + (1-\tau)\phi'_i$. This smooth evolution of target networks is key in our simulation-based setup, where abrupt Q-value changes may lead to erratic base station switching.

IV. SIMULATION RESULTS

A. Simulation Settings

In this section, we present numerical results to evaluate the performance of the proposed TD3-based model. Our simulations are conducted within an O-RAN environment, where M RUs serve K UEs. The RUs are uniformly spaced across a square service area of dimensions $L \times L$ m² illustrated in Fig.2. To investigate the impact of network size on model performance, we consider two different service area sizes.

Algorithm 1: TD3-Based Energy-Aware RU Control

Input: Initial network state s_0 , actor parameters θ , critic parameters ϕ_1, ϕ_2 , replay buffer \mathcal{D}

Output: Trained actor network μ_θ for RU sleep scheduling

```

1 for each episode do
2   Initialize environment and receive initial state  $s$ ;
3   for each time step  $t = 1, \dots, T$  do
4     Add exploration noise  $\eta_t \sim \mathcal{N}(0, \sigma^2)$ ;
5     Compute continuous action:  $a_c = \mu_\theta(s) + \eta_t$ ;
6     Discretize:  $a = f_d(a_c)$  where  $a_i = \mathbb{I}[a_{c,i} > 0.5]$ ;
7     Execute action  $a$  in the environment;
8     Receive reward  $r$  and next state  $s'$ ;
9     Store  $(s, a, r, s')$  into replay buffer  $\mathcal{D}$ ;
10    Sample a mini-batch  $(s_j, a_j, r_j, s'_j)$  from  $\mathcal{D}$ ;
11    Compute target action:  $\tilde{a}_j = f_d(\mu_{\theta'}(s'_j) + \epsilon)$ ;
12    Compute target Q-value:
         $y_j = r_j + \gamma \min_{i=1,2} Q_{\phi'_i}(s'_j, \tilde{a}_j)$ ;
13    Update critics  $\phi_1, \phi_2$  by minimizing:
         $\mathcal{L}(\phi_i) = \frac{1}{N} \sum_j (Q_{\phi_i}(s_j, a_j) - y_j)^2$ ;
14    if every  $d$  steps then
15      Update actor using deterministic policy gradient
16      ;
17      Soft-update target networks:
         $\phi'_i \leftarrow \tau\phi_i + (1-\tau)\phi'_i, \theta' \leftarrow \tau\theta + (1-\tau)\theta'$ ;
18     $s \leftarrow s'$ 

```

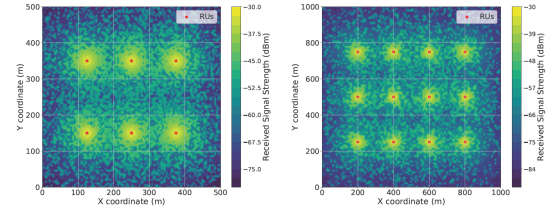


Fig. 2: illustrates the radio maps of 500×500 m² and 1000×1000 m² area.

This comparison allows us to assess how performance varies in different spatial environments. It is important to note that the DQN multi-action model is constrained to small service areas due to the exponentially growing action space in larger environments. Consequently, its training feasibility is limited when the network size increases, whereas the other models remain applicable across different service area scales. The UEs move at a speed, denoted as $v = v_{\text{avg}} \pm v_{\text{std}}$, where v_{avg} represents the mean speed and v_{std} denotes the standard deviation of the speed. The actual speed of each UE is randomly selected within this range. Furthermore, we define a movement probability distribution for UEs based on their location to ensure a periodic mobility pattern. This pattern dictates that UEs consistently move from the edge of the service area toward the center and then back to the edge, maintaining a structured and cyclic movement behavior. For the fading channel model, we employ the Urban Microcell (UMi) channel model, considering the conditions Line of Sight (LOS) and Non-Line of Sight (NLOS), expressed as:

For LOS conditions:

$$PL_{m,k}^{\text{LOS}} = \begin{cases} 32.4 + 21 \log_{10}(d_{m,k}) + 20 \log_{10}(f), & d_{m,k} \leq d_{\text{BP}}, \\ 32.4 + 40 \log_{10}(d_{m,k}) + 20 \log_{10}(f) - 9.5, & d_{m,k} > d_{\text{BP}}, \end{cases} \quad (10)$$

$$d_{\text{BP}} = \frac{4h_{\text{RU}}h_{\text{UE}}f}{c}, \quad (11)$$

where d_{BP} is the breakpoint distance, $PL_{m,k}$ represents the path loss, which follows the UMi path loss model.

For NLOS conditions:

$$PL_{m,k}^{\text{NLOS}} = 35.3 + 22.4 \log_{10}(d_{m,k}) + 21.3 \log_{10}(f) - 0.3(h_{\text{UE}} - 1.5), \quad (12)$$

where $d_{m,k}$ denotes the distance between the RU m and the UE k , f is the carrier frequency in GHz, and h_{UE} is the height of the UE in meters.

The LOS probability is determined by:

$$P_{\text{LOS}} = \min\left(\frac{18}{d_{m,k}}, 1\right) \left(1 - e^{-d_{m,k}/36}\right) + e^{-d_{m,k}/36}. \quad (13)$$

The NLOS probability is then given by $P_{\text{NLOS}} = 1 - P_{\text{LOS}}$.

Parameters	Value
Carrier frequency (f)	2 GHz
RU height (h_{RU})	15 m
UE height (h_{UE})	1.7 m
Network size (L)	[500,1000] m
Number of RUs (M)	[6, 12]
Number of UEs (K)	[10 - 80]
Minimum Data rate requirement (R_{min})	3 Mbps
Noise power (σ_n^2)	-174 dBm/Hz
Power amplifier (η)	0.5
Average speed of UE (v_{avg})	2 m/s
Standard deviation of UE speed (v_{std})	0.5 m/s
Fix active mode RU power (P^{active})	20 W
Fix sleep mode RU power (P^{sleep})	5 W
Maximum transmission power (P_{TX})	1 W / 30dBm
Mode transition power (P^{trans})	3 W

TABLE I: Simulation Parameters

During the training process, each episode consists of 200 time steps, with each time step corresponding to 1 second. At every time step, the agent determines the sleep mode status of the RUs, making operational decisions accordingly. The network energy consumption is then evaluated based on these decisions. As a result, the total simulation duration for each episode amounts to 200 seconds. In the TD3 model, both the actor and critic networks consist of four fully connected layers. The configuration of activation functions and layer sizes are detailed in Table I. Additionally, Batch Normalization (BN) is incorporated to enhance training stability. For the DQN models, both networks comprise five fully connected layers, with their detailed architectures also provided in Table II.

In the subsequent section, we present a comparative analysis of the proposed TD3 model against three baseline techniques for RU sleep mode management. The first baseline, termed

	Layer1	Layer2	Layer3	Layer4	Output Layer
Actor	BN+relu 512	relu 256	relu 128	None	sigmoid M
Critic	relu 512	relu 256	relu 128	None	linear 1
DQNSA	relu 512	relu 384	relu 256	relu 128	linear M^2
DQNMA	relu 512	relu 384	relu 256	relu 128	linear $2M$

TABLE II: Network Configurations

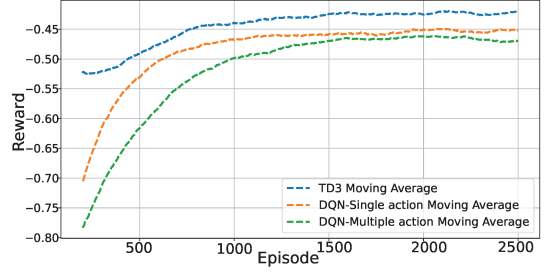


Fig. 3: illustrates the rewards of TD3, DQNSA and DQNMA in $500 \times 500 \text{ m}^2$ scenario

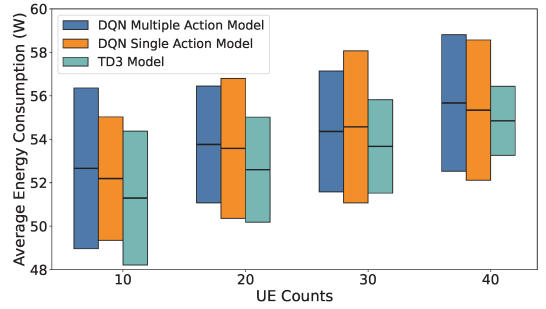


Fig. 4: illustrates the average energy consumption in $500 \times 500 \text{ m}^2$ scenario among 10 to 40 UEs with DQNMA, DQNSA and TD3 models.

”All Active Mode,” serves as a reference scenario where all RUs remain continuously active. The second baseline is the DQNSA model, which dynamically switches the sleep mode status of only one RU per time slot. The third baseline, referred to as the DQNMA model, simultaneously adjusts the sleep modes for all RUs within the network at each time interval.

B. Simulation Results

In Fig.3 illustrates the reward performance over 2500 episodes for the TD3, DQNSA and DQNMA models in $500 \times 500 \text{ m}^2$ area. Notably, the TD3 model consistently achieves the highest reward performance, demonstrating superior stability and convergence compare to both DQN models. The DQNSA model exhibits moderate performance with noticeable fluctuations, while the DQNMA model shows the lowest reward, indicating that increasing the complexity of actions within the DQN architecture does not necessarily translate into better reward outcomes in this scenario. In Fig.4 indicates the energy consumption performance in $500 \times 500 \text{ m}^2$ area for varying UE counts ranging from 10 to 40, is still compared among the previous three models. The figure distinctly shows the average energy consumption, indicated by the black line in the center of each bar, while the length of each bar represents the variance in energy consumption. With a total of 6 RUs installed in

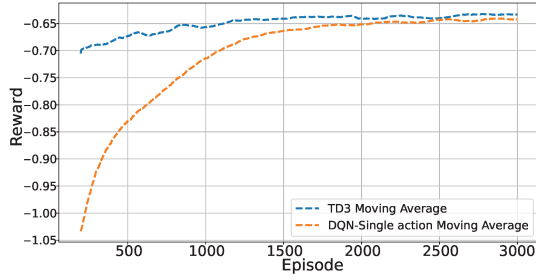


Fig. 5: illustrates the rewards of TD3 and DQNSA model in $1000 \times 1000 \text{ m}^2$ scenario

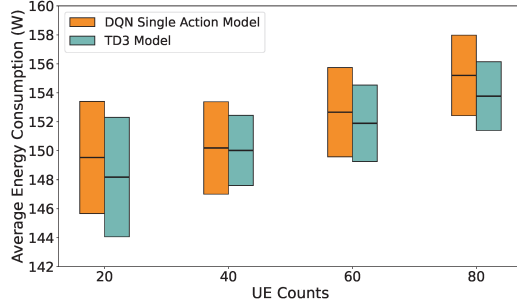


Fig. 6: illustrates the average energy consumption among 20 to 80 UEs in $1000 \times 1000 \text{ m}^2$ scenario with TD3 and DQNSA models.

this area, the maximum possible energy consumption reaches 126w when all RUs operate in active mode. The results clearly demonstrate that all three models achieve significant energy savings, exceeding 50% compared to the theoretical maximum. Specifically, the TD3 model achieving up to an additional 6% energy saving compared to the two DQN-based models. Conversely, the DQNMA model demonstrates the highest energy consumption, underscoring potential inefficiencies associated with more complex action spaces.

In Fig.5 shows the reward performance over an extended simulation environment from $500 \times 500 \text{ m}^2$ area to 1000 m^2 area. But only compare the TD3 model against the DQNSA model due to the excessive expansion of DQNMA action space (e.g. 2^{12}). In the results, the TD3 model still achieves higher and stable reward levels throughout all episodes. Furthermore, the TD3 model demonstrates faster and more efficient convergence toward optimal solutions. The Fig.6 illustrates the energy consumption between the TD3 and DQNSA model, covering UE counts from 20 to 80. Numerically, the TD3 model maintains lower energy consumption, approximately 144w at 20 UEs and up to around 152w at 80 UEs, significantly below the theoretical maximum consumption of 252 watts (more than 40%) with all 12 RUs active. However, the TD3 model can also achieve 5% over the DQNSA mode, further emphasizing the TD3 model in a complex and large-scale environment.

V. CONCLUSIONS

This paper proposed an energy-efficient framework for controlling RU sleep modes in O-RAN using advanced DRL

methods. Proposed TD3 algorithm was implemented to effectively handle the continuous action space inherent to RU state decisions, directly addressing the limitations encountered by discrete-action methods like DQN-based approaches. In comparison, the proposed TD3 algorithm demonstrated superior performance, consistently achieving higher stability, faster convergence, and greater energy efficiency. Numerical results clearly indicated that TD3 delivered up to 6% additional energy savings over the baseline DQN methods, particularly highlighting its scalability and effectiveness in larger and more dynamic network scenarios. Future research directions will focus on enhancing this TD3-based approach through Federated Learning (FL). This future work aims to leverage FL principles to further enhance scalability.

VI. ACKNOWLEDGMENT

This work has been supported by CHEDDAR: Communications Hub for Empowering Distributed Cloud Computing Applications and Research, funded by the UK EPSRC under grant numbers EP/Y037421/1 and EP/X040518/1, and by the Department of Science, Innovation and Technology, United Kingdom, under Grant Yorkshire Open-RAN (YORAN) TS/X013758/1.

REFERENCES

- [1] X. Liang, Q. Wang, A. Al-Tahmeesschi, S. B. Chetty, D. Grace, and H. Ahmadi, "Energy consumption of machine learning enhanced open ran: A comprehensive review," *IEEE Access*, vol. 12, pp. 81 889–81 910, 2024.
- [2] O-RAN Allience WG1, "O-RAN Architecture Description," October 2022, accessed: 2 Jan 2023. [Online]. Available: <https://orandownload.web.azurewebsites.net/specifications>
- [3] O-RAN Allience WG2, "A1 Interface: general aspects and principles 3.0," October 2022, accessed: 12 Dec 2022. [Online]. Available: <https://orandownload.web.azurewebsites.net/specifications>
- [4] A. I. Abubakar, O. Onireti, Y. Sambo, L. Zhang, G. Ragesh, and M. A. Imran, "Energy efficiency of open radio access network: A survey," in *2023 IEEE 97th Vehicular Technology Conference (VTC2023-Spring)*. IEEE, 2023, pp. 1–7.
- [5] J. Wu, Y. Zhang, M. Zukerman, and E. K.-N. Yung, "Energy-efficient base-stations sleep-mode techniques in green cellular networks: A survey," *IEEE communications surveys & tutorials*, vol. 17, no. 2, pp. 803–826, 2015.
- [6] C. Liu, B. Natarajan, and H. Xia, "Small cell base station sleep strategies for energy efficiency," *IEEE Transactions on Vehicular Technology*, vol. 65, no. 3, pp. 1652–1661, 2015.
- [7] E. Oh and K. Son, "A unified base station switching framework considering both uplink and downlink traffic," *IEEE Wireless Communications Letters*, vol. 6, no. 1, pp. 30–33, 2016.
- [8] J. Peng, P. Hong, and K. Xue, "Stochastic analysis of optimal base station energy saving in cellular networks with sleep mode," *IEEE Communications Letters*, vol. 18, no. 4, pp. 612–615, 2014.
- [9] J. Ye and Y.-J. A. Zhang, "Drag: Deep reinforcement learning based base station activation in heterogeneous networks," *IEEE Transactions on Mobile Computing*, vol. 19, no. 9, pp. 2076–2087, 2019.
- [10] H. Ju, S. Kim, Y. Kim, and B. Shim, "Energy-efficient ultra-dense network with deep reinforcement learning," *IEEE Transactions on Wireless Communications*, vol. 21, no. 8, pp. 6539–6552, 2022.
- [11] G. Jang, N. Kim, T. Ha, C. Lee, and S. Cho, "Base station switching and sleep mode optimization with lstm-based user prediction," *IEEE Access*, vol. 8, pp. 222 711–222 723, 2020.
- [12] S. Sun, C. Huang, G. Chen, P. Xiao, and R. Tafazolli, "Deep learning-based traffic-aware base station sleep mode and cell zooming strategy in ris-aided multi-cell networks," *IEEE Transactions on Cognitive Communications and Networking*, 2024.
- [13] Q. Wang, S. Chetty, A. Al-Tahmeesschi, X. Liang, Y. Chu, and H. Ahmadi, "Energy saving in 6g o-ran using dqn-based xapp," *arXiv preprint arXiv:2409.15098*, 2024.